

NOTICE WARNING CONCERNING COPYRIGHT RESTRICTIONS:

The copyright law of the United States (title 17, U.S. Code) governs the making of photocopies or other reproductions of copyrighted material. Any copying of this document without permission of its author may be prohibited by law.

NAMT

94-029

**The Effect of Applied Loads on the
Magnetostrictive Response of a
Terfenol-D-Type Material:
A Micromagnetic Analysis**

**Antonio DeSimone
Universita di Roma "Tor Vergata"**

Research Report No.94-NA-029

September 1994

Sponsors

**U.S. Army Research Office
Research Triangle Park
NC 27709**

**National Science Foundation
1800 G Street, N.W.
Washington, DC 20550**

University Libraries
Carnegie Mellon University
Pittsburgh PA 15213-3890

TMAU
P60-HP

THE EFFECT OF APPLIED LOADS ON THE MAGNETOSTRICTIVE RESPONSE OF A TERFENOL-D-TYPE MATERIAL: A MICROMAGNETIC ANALYSIS

Antonio DeSimone
Dipartimento di Ingegneria Civile
Università di Roma "Tor Vergata"
00133, Roma, ITALY

Introduction

Terfenol-D is a highly magnetostrictive material. Strains of the order of 2×10^{-3} are achieved at room temperature under reasonably low applied field strengths (1), and this renders Terfenol-D very promising for applications like active vibration control, precision machining, etc. As it is common for magnetic materials, the macroscopic properties of technological interest, such as the change of length of a magnetostrictive rod under the action of an external magnetic field, arise from the cooperative evolution of microscopic magnetoelastic domains. In order to understand and predict the macroscopic response of a given specimen to magneto-mechanical loads, it is therefore natural to try to analyze domain evolution at the microscopic scale, and then to characterize the macroscopic behavior by a suitable averaging procedure. In essence, our approach to the computation of virgin magnetization and magnetostriction curves is an attempt to turn the previous statement into an algorithm based on a precise mathematical formulation of the problem. Our method is based on micromagnetics (cfr. (2, 3) for a discussion of differences and similarities with other, more standard procedures): we arrive at predictions of the macroscopic response of a given specimen by averaging magnetizations and strains corresponding to energy minimizing configurations.

In this paper, we report on preliminary results of our efforts to model the magnetostrictive response of a Terfenol-D specimen. Typically, this material is grown by the Free Standing Zone method in the shape of cylindrical rods. When this technique is used, Terfenol-D grows along a [112] direction in twinned dendritic sheets. Due to the presence of growth-twins, which are oriented along low symmetry crystallographic directions, the domain patterns corresponding to stable configurations are rather complex. We study the interplay of crystallographic and magneto-

mechanical properties, and its influence on the macroscopic response to applied magnetic fields and loads on a model problem: we consider a two-dimensional geometry¹, and we assume the saturation magnetostrictive strains along the [111] and [100] directions to be equal. In particular, we analyze the role of applied stresses in selecting the energetically optimal domain patterns, and the implications on the magnetostrictive response. We aim at a quantitative analysis, and the assumptions above allow us to carry out our program in full mathematical rigor. For Terfenol-D, however, $\lambda_{100} \ll \lambda_{111}$. Hence the material we study is only Terfenol-D-like, and our quantitative predictions are, at this stage, only qualitative for Terfenol-D.

The energy functional

We describe the state of a magnetostrictive body occupying the region of space Ω by a pair of functions defined on Ω : the magnetization \mathbf{m} (a vector field of prescribed length, equal to the saturation magnetostriction m_s at the temperature of interest), and the strain \mathbf{E} (we recall that $\mathbf{E}(x) = (\nabla \mathbf{u}(x) + \nabla^T \mathbf{u}(x))/2$, where $\mathbf{u}(x)$ denotes the displacement of the point x of Ω). We are interested in minimizers of the free energy functional

$$F_{\mathbf{h},\mathbf{S}}(\mathbf{m},\mathbf{E}) = \int_{\Omega} (\varphi_{tot}(\mathbf{m}(x),\mathbf{E}(x)) - (\frac{1}{2}\mathbf{h}_m(x) + \mathbf{h}) \cdot \mathbf{m}(x) - \mathbf{S} \cdot \mathbf{E}(x)) dx ,$$

where \mathbf{h} is a uniform applied magnetic field, \mathbf{S} is a uniform stress applied at the boundary of Ω , \mathbf{h}_m is the demagnetizing field and $\varphi_{tot}(\mathbf{m},\mathbf{E}) = \varphi(\mathbf{m}) + [\mathbf{E} - \mathbf{E}_o(\mathbf{m})] \cdot \mathbf{C}[\mathbf{E} - \mathbf{E}_o(\mathbf{m})]/2$ (here φ is the magnetocrystalline anisotropy energy density, $\mathbf{E}_o(\mathbf{m})$ is the spontaneous strain corresponding to \mathbf{m} , and \mathbf{C} is the fourth order tensor of elastic moduli). We remark that the magnetoelastic energy term in $F_{\mathbf{h},\mathbf{S}}$ is obtained from more standard expressions (5) by elementary algebraic manipulation. Moreover, our energy functional does not contain an exchange energy term: indeed, it arises as an appropriate limit of the energy functional of micromagnetics, suitable for the study of sufficiently large specimens (6). It is instructive to rewrite the energy $F_{\mathbf{h},\mathbf{S}}$ in an equivalent form, which makes more transparent the role of the applied stresses in the selection of minimum energy configurations. For fixed \mathbf{h} and \mathbf{S} , the energy

$$G_{\mathbf{h},\mathbf{S}}(\mathbf{m},\mathbf{E}) = \int_{\Omega} (\varphi_{s,tot}(\mathbf{m}(x),\mathbf{E}(x)) - (\frac{1}{2}\mathbf{h}_m(x) + \mathbf{h}) \cdot \mathbf{m}(x)) dx ,$$

¹This choice allows us to compare our results with those derived from the qualitative model described in (1), and with the computational results reported in (4): in both papers the authors consider a two-dimensional model.

where $\varphi_{s,wr}(\mathbf{m}, \mathbf{E}) = \varphi_s(\mathbf{m}) + [\mathbf{E} - (\mathbf{E}_o(\mathbf{m}) + \mathbf{E}_s)] \cdot \mathbf{C} [\mathbf{E} - (\mathbf{E}_o(\mathbf{m}) + \mathbf{E}_s)] / 2$, $\mathbf{E}_s = \mathbf{C}^{-1} \mathbf{S}$, and $\varphi_s(\mathbf{m}) = \varphi(\mathbf{m}) - \mathbf{S} \cdot \mathbf{E}_o(\mathbf{m})$, differs from $F_{h,s}$ by a constant, and hence it leads to an equivalent minimization problem. However, the expression of $G_{h,s}$ clearly shows that applying the prestress \mathbf{S} affects the spontaneous strain corresponding to \mathbf{m} , but it also effectively modifies the anisotropy energy term.

In our calculations, we take Ω to be the two-dimensional domain shown in Fig. 1, and we assume that \mathbf{m} always lie in the plane of Ω . The picture shows that Ω consists of thin² growth-twinned parallel platelets, and the orientations of the crystallographic axes and of the magnetically easy directions are shown in the inset for both the parent and the twin phase. With the exception of the values for the saturation magnetostriction (we take $\lambda_{100} = \lambda_{111} = 1.2 \times 10^{-3}$), we essentially take for the material parameters the values reported in the experimental literature for Terfenol-D (7). The applied field is parallel to the [112] direction, and the only non-zero component of \mathbf{S} consists of a compressive normal stress σ along the same direction.

We close this section with a crucial observation, due to James and Kinderlehrer (8). Due to the absence of the exchange energy, it may be energetically advantageous for our system to let the size of the magnetoelastic domains shrink to zero. This is, for example, the case for $h=0$ and $\mathbf{S} \neq 0$, and the inset in Fig. 1 shows schematically the corresponding magnetic domains (their width is proportional to $1/k$, with k a positive integer). As k tends to infinity, the energy tends to its infimum $I_{0,s}$, and there is no "classical" magnetization-deformation pair whose energy is exactly $I_{0,s}$. Thus energy minimization may lead to microstructures, i.e., infinitely refining minimizing sequences (parametrized by the width of the domains) or, in a language reminiscent of Néel's terminology (9), microscopic mixtures of magnetic phases. This is not surprising: $G_{h,s}$ captures the limiting behavior of increasingly larger bodies. It is well known that, typically, as the size of a specimen tends to infinity, the ratio between the size of the domains and the size of the specimen tends to zero. Since in our approach this limiting process is observed by mapping the domain patterns on a reference body of fixed size (6), infinite refinement occurs. For the purpose of analyzing energy minimizing microstructures, a quantity of interest is the (limiting) local average $\langle \mathbf{m} \rangle$ corresponding to a given sequence of magnetizations $\{\mathbf{m}_k\}$, i.e., its weak limit. This is obtained, at each point x of Ω , by taking the average of \mathbf{m}_k over a ball of radius ρ centered at x , then by letting k tend to infinity, and then ρ to zero. For a "classical" magnetization field \mathbf{m} , which can be identified with the trivial sequence $\{\mathbf{m}_k = \mathbf{m}\}$ identically, clearly $\langle \mathbf{m} \rangle = \mathbf{m}$.

²In each platelet, we take the demagnetizing factors to be zero in the [112] direction, and one in the orthogonal direction.

Energy minimizing microstructures

In the computation of energy minimizing microstructures, several issues need to be addressed. Here we will focus on the least technical of them, namely, the evaluation of the anisotropy energy associated with an energetically optimal microstructure, which is also the most relevant issue in assessing the influence of applied stresses on the magnetostrictive response. Indeed, φ_s is defined only on a sphere of radius m_s , i.e., only for classical magnetizations. Introducing the convexification $\varphi_{s,eff}$ of φ_s , we can compute the lowest anisotropy energy density attainable by a microstructure with a given local average magnetization. More precisely:

$$\varphi_{s,eff}(\mathbf{u}) = \inf \left\{ \frac{1}{\lambda} \sum_{i=1}^3 \lambda_i \varphi_s(\mathbf{v}_i), \text{ with } \frac{1}{\lambda} \sum_{i=1}^3 \lambda_i \mathbf{v}_i = \mathbf{u}, \lambda_i \geq 0 \right\},$$

where $\lambda = \sum \lambda_i$ and, moreover \mathbf{u} and \mathbf{v}_i are in the plane of Ω (here we are using the fact that, in the problem at hand, the restriction of $\varphi_{s,eff}$ to the plane of Ω coincides with the convexification of the restriction of φ_s to the same plane). Using the results of (3,6), we find that the local average magnetization of energy minimizing microstructures satisfies the equation

$$\frac{\partial}{\partial \langle \mathbf{m} \rangle} \varphi_{s,eff}(\langle \mathbf{m} \rangle) - (\mathbf{h} + \mathbf{h}_{\langle \mathbf{m} \rangle}) = \beta \langle \mathbf{m} \rangle$$

where β is a Lagrange multiplier and $\mathbf{h}_{\langle \mathbf{m} \rangle}$ is the demagnetizing field generated by $\langle \mathbf{m} \rangle$ (note that we needed to pass to a formulation in terms of microstructures in order to find a meaningful version of the Euler-Lagrange equations of our problem). The equation above takes two different forms in the parent and in the twin phase. However the solution in the twin phase is easily obtained from the one in the parent phase by symmetry, and in what follows we will concentrate on the parent phase only.

In Fig. 2 we have schematically shown the level curves of the function $\varphi_{s,eff}$ of the parent phase for several values of σ . Moreover, for $\sigma = 0$ and for $\sigma = 5$ MPa, we have plotted the local average magnetization in the parent phase for the energetically optimal microstructures corresponding to field strengths in the interval $[0, \infty)$. The magnetization curves, shown in Fig. 3 are immediately obtained from these plots by averaging the [112] component of $\langle \mathbf{m} \rangle$ over the whole specimen. Moreover, we can use the plots of Fig. 2 to reconstruct those features of the microstructures which are necessary for the computation of the magnetostriction curves. The points

on the circles represent saturated states, and for each of them the corresponding minimum energy deformation is $\mathbf{E}=\mathbf{E}_o(\mathbf{m})+\mathbf{E}_S$. The local average magnetizations whose representative points fall in the interior of the circles correspond to microstructures. Using the level curves of $\varphi_{s,\sigma}$ we can find for each of them, say $\langle\mathbf{m}\rangle$, points on the circles, say \mathbf{m}_i , such that $(1/\lambda)\sum\lambda_i\varphi_s(\mathbf{m}_i)=\varphi_{s,\sigma}(\langle\mathbf{m}\rangle)$, and $(1/\lambda)\sum\lambda_i\mathbf{m}_i=\langle\mathbf{m}\rangle$. Thus we can generate a microstructure with anisotropy energy density $\varphi_{s,\sigma}(\langle\mathbf{m}\rangle)$ by constructing suitable arrangements of magnetic domains with magnetizations \mathbf{m}_i and local volume fractions (asymptotically equal to) λ_i/λ , and by letting the size of these domains tend to zero. In each domain, we take $\mathbf{E}=\mathbf{E}_o(\mathbf{m}_i)+\mathbf{E}_S$, and we compute the magnetostriction curves by taking averages of the [112] components of the strains over the whole specimen (Fig. 4).

In concluding this section, we briefly mention some of the more technical issues underlying our analysis, which will be discussed elsewhere in more detail. If no additional energy (either demagnetizing or magnetoelastic contributions) arises from the presence of discontinuities of the magnetization within each of the growth-twinned lamellae, then the procedure outlined above correctly leads to the computation of the "minimizers" of $G_{h,s}$. In particular, we observe that in the previous developments the magnetoelastic contribution is always zero, since we have taken $\mathbf{E}(x)=\mathbf{E}_o(\mathbf{m}(x))+\mathbf{E}_S$ everywhere in the specimen. However this is admissible only if $\mathbf{E}_o(\mathbf{m})$ satisfies the kinematical compatibility conditions of linear elasticity. This is the case in our problem³, precisely because we have assumed $\lambda_{100}=\lambda_{111}$.

Discussion

We have presented a quantitative analysis of the effect of applied stresses on the macroscopic response to applied magnetic fields of a growth-twinned magnetostrictive specimen. Our method is based on a rigorous minimization procedure, and it is an attempt at bridging, at least partially, the existing gap between theoretical predictions and experimental observations of the behavior of Terfenol-D. Our ideal material shares many of the properties of Terfenol-D, and its response exhibits marked similarities with the experimental observations reviewed in (1). However, the two-dimensional character of our computed domain patterns, and the assumption $\lambda_{100}=\lambda_{111}$ lead to magnetostriction curves in directions orthogonal to [112] in contrast with experimental observations (11): the $[\bar{1}\bar{1}1]$ curve for the loaded specimen is obtained from the [112] curve by a change of sign. The conclusions we draw from our analysis are the following. Our material achieves strains

³We note that kinematic compatibility across the growth-twinned boundaries is satisfied asymptotically (10): we construct transition layers whose width shrinks to zero when the width of the domains in the platelets tends to zero, and whose energy contribution becomes negligible in the limit.

comparable with those of a Terfenol-D rod, even though we take for λ_{111} a comparatively small value, in agreement with the belief that reducing the anisotropy of Terfenol-D would lead to improved performance (12). Moreover, the sharp difference in the magnetostrictive response at low and high levels of prestress is explained by a change of symmetry of the anisotropy energy $\varphi_{s,\sigma}$. The essentially cubic symmetry of the top two graphs in Fig. 2 degenerates into the essentially uniaxial symmetry of the lower two as σ increases. In fact, the magnetostriction curve for the loaded specimen shown in Fig. 4 is typical of uniaxial specimens, when a field is applied along a direction intermediate between the easy and the hard axis (2). Some preliminary calculations suggest that assuming $\lambda_{100} \ll \lambda_{111}$, as it is more realistic for Terfenol-D, and allowing for genuinely three-dimensional domain patterns should lead to predictions in better agreement with the experimental observations, although through more elaborate computations.

Acknowledgements

This paper was written while the author was a Postdoctoral Associate at the Center for Nonlinear Analysis (Department of Mathematics, Carnegie Mellon University). Partial support for this research was provided by the ARO and the NSF through a grant to the CNA.

References

1. A.E. Clark, High power rare earth magnetostrictive materials. In *Recent Advances in Adaptive and Sensory Materials*, (C.A. Rogers and R.C. Rogers eds.), p.387, Technomic, (1992).
2. A. DeSimone, Magnetoelastic solids: macroscopic response and microstructure evolution under applied magnetic fields and loads. *Journal of Intelligent Material Systems and Structures*, to appear (1994).
3. A. DeSimone, Magnetization and magnetostriction curves from micromagnetics. *J. Appl. Phys.*, to appear (1994).
4. L. Ma and D. Kinderlehrer, MMM-Intermag 1994, Albuquerque, June 1994.
5. A.E. Clark, Magnetostrictive Rare Earth-Fe₂ compounds. In *Ferromagnetic Materials*, Vol. 1, (E.P. Wohlfarth ed.), p.532, North-Holland (1980).
6. A. DeSimone, Energy minimizers for large ferromagnetic bodies. *Arch. Rat. Mech. Anal.*, 125, 99 (1993).
7. J.P. Teter, A.E. Clark and O.D. McMaster, Anisotropic magnetostriction in Tb_{0.27}Dy_{0.73}Fe_{1.95}. *J. Appl. Phys.*, 61, 3787 (1987).

8. R.D. James and D. Kinderlehrer, Frustration in ferromagnetic materials. *Cont. Mech. Therm.*, 2, 215, (1990).
9. L. Néel, Les lois de l'aimantation et de la subdivision en domaines élémentaires d'un monocristal de fer. *J. Phys. Rad.*, 5, 241, (1944).
10. R.D. James and D. Kinderlehrer, Theory of magnetostriction with applications to $Tb_xDy_{1-x}Fe_2$. *Phil. Mag. B*, 68, 237, (1993).
11. J.P. Teter, M. Wun-Fogle, A.E. Clark and K. Mahoney, Anisotropic perpendicular axis magnetostriction in twinned $Tb_xDy_{1-x}Fe_{1.95}$. *J. Appl. Phys.*, 67, 5004, (1990).
12. J. Cullen, Lecture at the Acta Met. Meeting on "Novel Magnetic Properties and Structures", Santa Fe, June 1994.

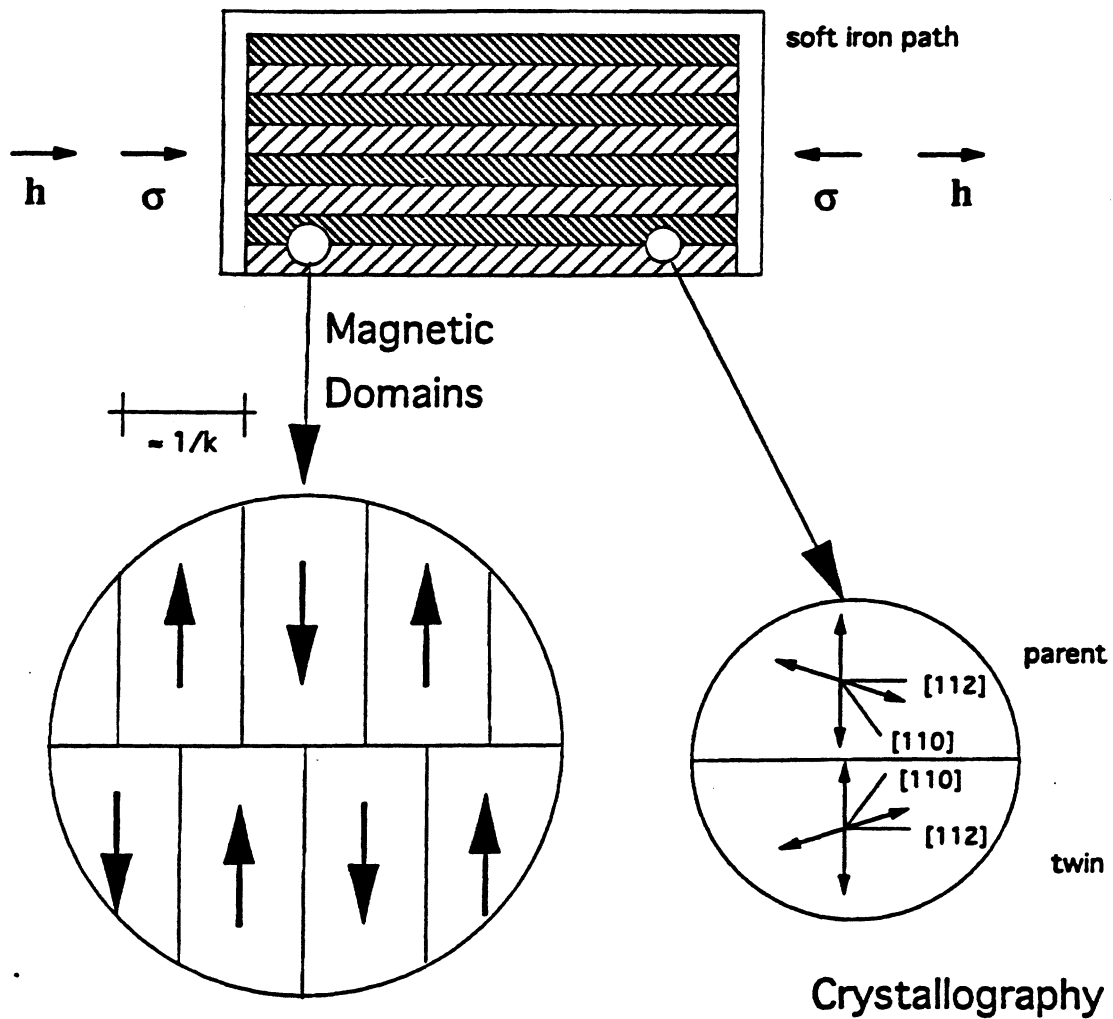


Fig. 1. The geometry for our problem. In the insets, the magnetically easy axes and the crystallographic directions for parent and twin phases, and a schematic representation of the magnetic domain patterns corresponding to the optimal microstructures for $h=0$ and $\sigma \neq 0$. The width of the domains is proportional to $1/k$, and the representation becomes "exact" in the limit as k tends to infinity.

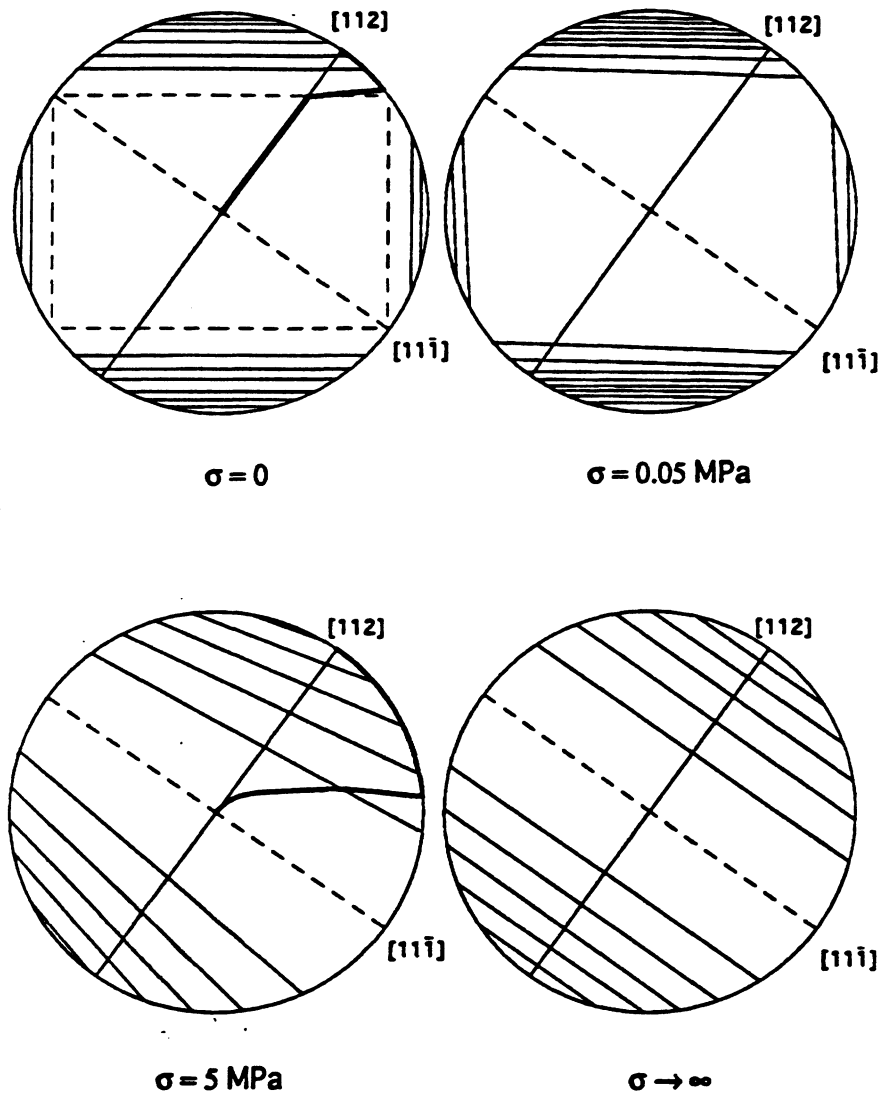


Fig. 2. A schematic representation of the level curves of $\varphi_{s,\sigma}$ in the parent phase, for several values of the prestress. The dashed lines correspond, for each σ , to the minima of $\varphi_{s,\sigma}$. Also shown are the plots of the local average magnetization in the parent phase for $\sigma = 0$ and 5 MPa, and field strength in the interval $[0, \infty)$.

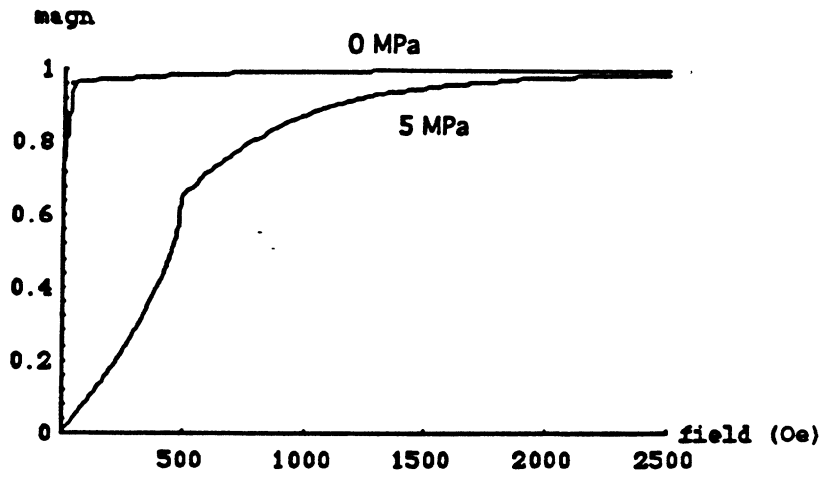


Fig. 3. [112] virgin magnetization curves.

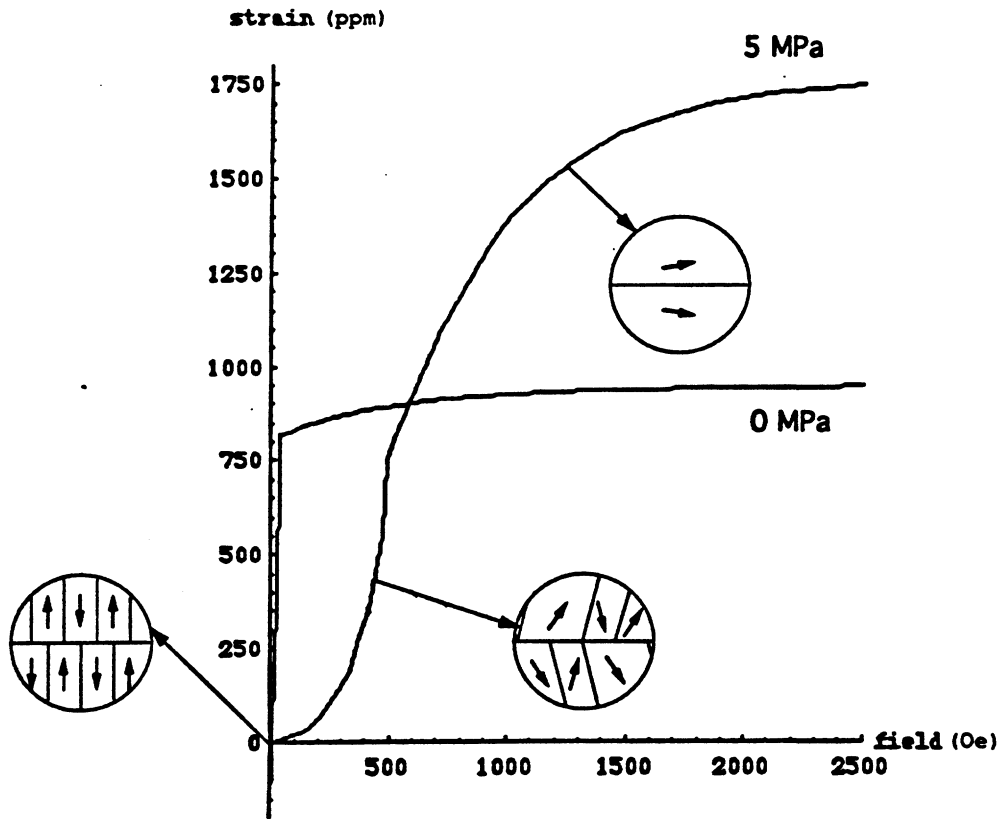


Fig. 4. [112] virgin magnetostriction curves, and a schematic representation of the underlying magnetic domain structures for $\sigma = 5$ MPa

MAR 25 2004

Carnegie Mellon University Libraries



3 8482 01375 7667